HHS Public Access

Author manuscript

Math Biosci. Author manuscript; available in PMC 2016 December 01.

Published in final edited form as:

Math Biosci. 2015 December ; 270(0 0): 224–236. doi:10.1016/j.mbs.2015.08.020.

Comparison of Mathematical Frameworks for Modeling Erythropoiesis in the Context of Malaria Infection

Luis L. Fonseca and **Eberhard O. Voit**

The Wallace H. Coulter Department of Biomedical Engineering, Georgia Institute of Technology and Emory University, 950 Atlantic Drive, Atlanta, Georgia, 30332-2000, USA

Abstract

Malaria is an infectious disease present all around the globe and responsible for half a million deaths per year. A within-host model of this infection requires a framework capable of properly approximating not only the blood stage of the infection but also the erythropoietic process that is in charge of overcoming the malaria induced anemia. Within this context, we compare ordinary differential equations (ODEs) with and without age classes, delayed differential equations (DDEs), and discrete recursive equations (DREs) with age classes. Results show that ODEs without age classes are fair approximations that do not provide a crisp temporal representation of the processes involved, and inclusion of age classes only mitigates the problem to some degree. DDEs perform well with respect to generating the essentially fixed delay between cell production and cell removal due to age, but the inclusion of any other processes, such as sudden blood loss, becomes cumbersome. The framework that was found to perform best in representing the dynamics of red blood cells during malaria infection is a DRE with age classes. In this model structure, the amount of time a cell remains alive is easily controlled, and the addition of age dependent or independent processes is straightforward. All events that populations of cells face during their lifespan, like growth or adaptation in differentiation or maturation rate, are properly represented in this framework.

Keywords

Within-host model; Malaria; Erythropoiesis; Discrete recursive equation; ODE; DDE

1. Introduction

Malaria is a worldwide infectious disease responsible for over half a million deaths per year [1] and for the perpetuation of genetic diseases like thalassemias, sickle-cell disease, and G6P dehydrogenase deficiency due to heterozygous advantage [2; 3; 4]. Malaria is caused by parasitic protozoans belonging to the genus *Plasmodium* and is transmitted by female *Anopheles* mosquitoes [5]. Upon entering the host, the protozoan takes temporary refuge in the liver where it multiplies and may remain dormant for several months, if not years. When

the parasite leaves the liver, it starts infecting red blood cells (RBCs), where it replicates. This stage ultimately causes most symptoms of malaria. Under normal healthy conditions, RBCs exhibit an almost deterministic lifespan with relatively small variation. However, during the blood stage infection, the parasitemia level increases and the number of erythrocytes plummets, thereby causing an increasing demand on erythropoiesis to replace lost cells. Erythropoiesis is regulated by negative feedback through erythropoietin, such that a hypoxia-induced increase in the concentration of erythropoietin promotes survival, proliferation and differentiation of erythroid progenitor cells. During the erythropoietic process, the erythroid progenitor cells undergo a number of mitotic events while differentiating through the several stages. Each differentiation stage is characterized by a specific duration and a fixed number of mitotic events, until ultimately a polychromatic erythroblast has formed. Concomitant with the destruction of RBCs, malarial infection also causes dysregulation of the erythropoietic process, due to interference with regulating cytokines and the production of the malaria pigment, hemozoin. This dysregulation is characterized by a failure to up-regulate RBC production properly, thereby resulting in anemia [6; 7; 8; 9].

The development of mathematical models characterizing the dynamics between hosts and malaria parasites requires an effective framework capable of addressing the dynamical regulation of RBC production, the parasite's life cycle characteristics, and interventions by the immune system [29]. Specifically, in order to capture the dynamics of erythropoiesis properly, a modeling framework needs to be able to address the adaptability of the cell differentiation process whose total duration, as well as the number of cell divisions between one stage and the next, respond to current needs. In principle, such features can be approximated with ordinary differential equations (ODEs) and mass action representations of the transitions between stages [30]. However, this framework does not properly capture the delays that cells encounter between entering and exiting a given stage of differentiation, because ODEs implicitly assume that removal from any of the differentiation stages is a probabilistic event. Delay differential equations (DDEs) are able to capture this delay, but the framework is rather inflexible, and any attempts to account for other processes of cell removal from a pool before the end of the time delay become cumbersome. Delays can also be generated in ODE models per approximation [10; 11] or by an explicit representation of the age-structure of cell populations within each stage [12]. Nonetheless, the issue of properly capturing the aging process, that is, the movement of cells from one age class to the next, still persists, as in the case of population models without age- structures. By contrast, discrete, recursive, age-structured models using difference equations (DREs) produce the required delays with relative ease, and if a transition matrix formulation is used, one can readily ensure that all cells in a given age class move to the next class at the correct time. In this paper, we compare these four alternative approaches and highlight their advantages and disadvantages.

Both malaria blood stage infections and hematopoietic processes have been the subject of numerous modeling activities, using not only ODEs [13; 14; 15; 16], but also DDEs [17; 18; 19], discrete equations [12] and PDEs [20; 21; 22]. However, to the best of our knowledge, the different approaches have not been compared in a systematic manner that highlights the advantages and disadvantages of each framework.

2. Methods

Malaria is obviously an exceedingly complex disease, and even a cursory discussion is beyond the scope of this article. Nonetheless, it is necessary to highlight some details of immediate relevance to modeling erythropoiesis.

Malaria parasites in the blood, known as merozoites, only replicate within RBCs and, depending on the *Plasmodium* species, may show a preference for cells of a given age. Once inside the RBC, the parasite completes its life cycle in 24 to 72 hours, depending on its species. At the end of the life cycle, the RBC membrane ruptures, and a new brood of merozoites is released into the blood stream. For each infected RBC, between 8 and 32 new merozoites [23] may be produced, again depending on the species. This ongoing process of RBC invasion and rupture leads to a decrease in the number of RBCs, to which the erythropoietic system responds. This system generates RBCs from multipotent hematopoietic stem cells in the bone marrow through several stages of differentiation and maturation. The process is controlled by hormones, like erythropoietin, that act by changing the rate of differentiation and level of proliferation. In essence, cells of each stage will, after a certain amount of time that is needed for differentiation and maturation, move into the next stage, while simultaneously undergoing a population expansion, so that more cells leave each stage than entered it. These same cells can also be subject to apoptosis. Thus, each stage may be characterized by two properties: the differentiation time and the amplification factor. In cells exclusively undergoing maturation, the amplification factor is 1. Since both of these properties depend on hormones, an appropriate modeling framework should allow for dynamical changes in these two properties, as they are encountered in malaria (for a review, see [24]). Once matured, RBCs have an essentially fixed life span of about 120 days in humans [25]; also, they do not grow or proliferate. However, a small percentage of seemingly healthy RBCs is removed throughout their lifetime in an apparently random manner. If an RBC is infected by *Plasmodium*, it bursts after one to three days, depending on the parasite species.

In order to investigate the best framework to model the malaria blood stage infection, the components were separated into two groups: cells with fixed lifespans (infected and non-infected RBCs) and cells with variable lifespans (erythropoietic progenitor and precursor cells).

2.1. Modeling the aging process of infected and non-infected RBCs

Three frameworks were compared for their ability to generate a fixed delay between cell production and removal: A) delay differential equations (DDEs); B) ordinary differential equations (ODEs) with age classes; and C) discrete recursive equations (DREs) with age classes (Figure 1). In order to render the comparison fair, the three systems were parameterized so that they exhibit external and internal equivalence as much as possible [26]. To be specific, a delay of 6 time units was chosen. This setting is explicitly enforced in the DDE by setting a delay of $\tau=6$, and the number of age classes in the ODE and discrete systems is set, accordingly, to $n=6$. Accordingly, the time-step of the discrete framework is defined as 1 unit. The influx of cells (F_{in}) into each of the three models is arbitrarily set to 2.

The DDE framework (Fig. 1A) is therefore modeled as

$$\frac{dX}{dt}=F_{in}(t)-F_{out}(t), \quad (1.1)$$

where the efflux of cells, F_{out}, is given by the number of cells that had entered the system τ time-units earlier:

$$\frac{dX}{dt}=F_{in}(t)-F_{in}(t-\tau) \quad (1.2)$$

With this formulation and with the initial condition $F_{in}(t) = 2$, for $-\tau \le t \le 0$, the steady-state is determined by the initial state of $X(0)$. We set this steady state to 12 to be consistent with all other frameworks.

The ODE framework with age-classes (Fig 1B) is formulated as:

$$\frac{dx_1}{dt}=F_{in}(t)-k\cdot x_1 \quad (2.1)$$

$$\frac{dx_i}{dt}=k\cdot x_{i-1}-k\cdot x_i, \quad i=2,3,4,..,n \quad (2.2)$$

For fair comparisons with other frameworks, k must equal n/τ, which enforces that cells remain in the system on average for τ time units. The total number of cells present in the system at any time point t is given by

$$X(t)=\sum_i x_i(t). \quad (3)$$

With a $n=6$, $\tau=6$ and $F_{in}(0)=2$, this framework has a steady-state $X=12$.

The DRE framework with age classes (Fig 1C) is formulated as:

$$\vec{X}_{t+1}=V\cdot\vec{X}_t+\begin{bmatrix}F_{in}(t)\\0\\0\\0\\0\\0\end{bmatrix}, \quad V=\begin{bmatrix}0&0&0&0&0&0\\1&0&0&0&0&0\\0&1&0&0&0&0\\0&0&1&0&0&0\\0&0&0&1&0&0\\0&0&0&0&1&0\end{bmatrix} \quad (4)$$

As in the case of the ODE with age-classes, the total number of cells present at a particular time point t equals the sum of the elements of $\vec{X}_t$:

$$X_t=\sum_i x_{i,t}. \quad (5)$$

The steady-state for $F_{in}(0)=2$ is again $X_\infty=12$.

To test the effect of a changing cell production in the models above, $F_{in}(t)$ was shifted from 2 to 5 for the time period $t\in$]5,7] and returned to 2 for $t\in$]7,20]:

$$F_{in}(t) = \begin{cases} 2 \ for\ t \in [0,5] \\ 5 \ for\ t \in (5,7] \\ 2 \ for\ t \in (7,20] \end{cases} \quad (6)$$

2.2. Modeling premature removal of infected and non-infected RBCs

The addition of a process that removes cells independently of their age is modeled as depicted in Figure 2. All parameters are kept at the same values as in Section 2.1. The first-order rate of premature removal of cells, k_2, was chosen arbitrarily as 1/12.

Adding an extra process of removal of cells in the DDE framework (Fig. 2A) leads to the formulation

$$\frac{dx}{dt} = F_{in}(t) - F_{in}(t-\tau) - k_2 \cdot X. \quad (7.1)$$

While at first seemingly appropriate, this representation does not accurately represent the desired system. The reason is the following. The term $-F_{in}(t-\tau)$ removes all cells that had entered the pool τ time units before. However, inclusion of the term $-k_2 \cdot X$ represents an instantaneous removal of cell that is proportional to the current pool size. The results is that some of the cells are removed twice. It is possible to estimate how many cells are removed by the additional term while they were allegedly in the system. In fact, by subtracting this quantity from the second loss term, $F_{in}(t-\tau)$, one can correct for the double removal and thus determine the approximate number of cells that remain in the pool at any given time. Specifically, the number of cells removed by the $-k_2 \cdot X$ term between $t-\tau$ and t is given by the integral

$$\int_{t-\tau}^{t} k_2 \cdot X = F_{in}(t-\tau) \cdot \left(1 - e^{-k_2 \cdot \tau}\right). \quad (8)$$

Adding this number back into the DDE framework (Eq. 7.1) corrects the problem:

$$\frac{dX}{dt} = F_{in}(t) - F_{in}(t-\tau) - k_2 \cdot X + F_{in}(t-\tau) \cdot \left(1 - e^{-k_2 \cdot \tau}\right) \quad (7.2)$$

Rearranging terms yields

$$\frac{dX}{dt} = F_{in}(t) - k_2 \cdot X - F_{in}(t-\tau) \cdot e^{-k_2 \cdot \tau}. \quad (7.3)$$

Comparative results of simulations of cell numbers with (Eq. 7.3) and without (Eq. 7.1) this correction will be shown in the *Results* Section.

For later comparisons of modeling frameworks, a process of cell removal from all age-classes ($-k_2 \cdot x_i$) was introduced in the ODE framework (Fig 2B), leading to

$$\frac{dx_1}{dt} = F_{in}(t) - k \cdot x_1 - k_2 \cdot x_1 \quad (9.1)$$

$$\frac{dx_i}{dt} = k \cdot x_{i-1} - k \cdot x_i - k_2 \cdot x_i, \qquad i = 2, 3, 4 \ldots n \quad (9.2)$$

Similarly, a process of cell removal was introduced for all age classes in the DRE framework with age-classes (Fig. 2C):

$$\vec{X}_{t+1} = V \cdot \vec{X}_t + \begin{bmatrix} F_{in}(t) \cdot (1-k_2) \\ 0 \\ 0 \\ 0 \\ 0 \\ 0 \end{bmatrix}, V = \begin{bmatrix} 0 & 0 & 0 & 0 & 0 & 0 \\ 1-k_2 & 0 & 0 & 0 & 0 & 0 \\ 0 & 1-k_2 & 0 & 0 & 0 & 0 \\ 0 & 0 & 1-k_2 & 0 & 0 & 0 \\ 0 & 0 & 0 & 1-k_2 & 0 & 0 \\ 0 & 0 & 0 & 0 & 1-k_2 & 0 \end{bmatrix} \quad (10)$$

As in Section 2.1, all systems were started at their original steady-states and tested by increasing cell production, $F_{in}(t)$ from 2 to 5 for $t \in (5,7]$:

$$F_{in}(t) = \begin{cases} 2 & for\ t \in [0,5] \\ 5 & for\ t \in (5,7] \\ 2 & for\ t \in (7,30] \end{cases} \quad (11)$$

2.3. Modeling RBC progenitor and precursor cells

Models describing the dynamics of progenitor cells are more complicated than for RBCs, because progenitor cells differ in their lifespans and furthermore proliferate, so that the overall RBC production process must include an appropriate amplification factor. Figure 3 indicates how this amplification enters the different frameworks. Panel (A) shows a single ODE with internal amplification (ODE IA); in this case, cells enter the pool as before, multiply inside the pool, and the number of cells leaving the pool is proportional to the pool size. Panel (B) depicts a slightly different scenario. Here, the amplification occurs outside the pool, that is, during the transition from one state to the next (ODE EA). In panel (C) the amplification occurs during the migration of cells from one age class to the next (ODE AC). Finally, panel (D) represents the corresponding discrete system with age classes and amplification during the transitions between age classes (DRE).

As before, all frameworks are parameterized with as much internal and external equivalence as possible. In particular, we set τ=6 (ODE IA, ODE EA and ODE AC; Fig. 3A, B, and C), n=6 (ODE AC and DRE; Fig. 3C and D), and F_{in}=2 for all cases. Additionally, the overall amplification factor, A_f, is arbitrarily set to 4 in all frameworks and, depending on the process, the amplification at the various steps is adjusted accordingly, as it is detailed below.

In the ODE system with internal growth (ODE IA, Fig. 3A) a single ODE is tested with an influx of F_{in}, and growth is modeled by assuming that cells within this pool grow with a rate of k_A. The age-dependent removal (F_{out}) of cells is modeled with a first-order process, where the rate constant of k_1 set to $1/\tau$. Thus, the system is formulated as

$$\frac{dX}{dt}=F_{in}(t)-k_1\cdot X+k_A\cdot X. \quad (12)$$

Here, the rate of growth, k_A, is estimated from the overall amplification factor, A_f, at the steady-state, $\frac{dX}{dt}=0$. At this state, the number of cells, X_{ss}, can be computed as

$$F_{in}(t)-k_1\cdot X_{SS}+k_A\cdot X_{SS}=0, \quad (13.1)$$

$$X_{SS}=\frac{F_{in}}{k_1-k_A}. \quad (13.2)$$

F_{in} cells enter the system, and these multiply so that, at the steady-state, A_f as many cells leave the pool. Thus,

$$F_{out}=A_f\cdot F_{in}, \quad (14.1)$$

which leads to

$$k_1\cdot X_{SS}=A_f\cdot F_{in}. \quad (14.2)$$

Combining Eqs. (13.2) and (14.2) yields

$$k_1\cdot\frac{F_{in}}{k_1-k_A}=A_f\cdot F_{in}, \quad (15.1)$$

$$k_A=k_1-\frac{k_1}{A_f}. \quad (15.2)$$

With this result, the number of cells present at the steady-state can be recalculated from Eqs. (13.2) and (15.2) as

$$X_{SS}=\frac{F_{in}}{k_1-k_A}=\frac{A_f\cdot F_{in}}{k_1}=A_f\cdot F_{in}\cdot\tau. \quad (13.3)$$

The ODE model with external amplification (ODE EA, Fig 3B) is set up in the following manner:

$$\frac{dX}{dt}=F_{in}\cdot A_{in}-k_1\cdot X. \quad (16.1)$$

Expressed in words, the flux entering the pool is amplified by the amplification factor A_{in}, while the flux leaving the pool is defined as $k_1\cdot X$, which corresponds to a typical transport and dilution process. However, when this process is used as influx to another pool, it is multiplied with the amplification factor A_{out}. To ensure that the overall amplification is the same as for other models, we enforce

$$A_{in} \cdot A_{out} = A_f \quad (16.2)$$

This amplification strategy (Eq. 16.1–16.2) allows slight variations for the determination of A_{in} and A_{out}, while still enforcing Eq. (16.2). The most straightforward definition is presumably

$$A_{in} = A_{out} = \sqrt{A}. \quad (17)$$

While in a sense natural, a system with this setting turns out to have a slow response time. An improvement is obtained when A_{in} and A_{out} are defined as proposed by Schirm *et al.*[27] and shown in Eqs. (18.1–18.2):

$$A_{in} = \begin{cases} \frac{A_f - 1}{log_2(A_f)} & for\ A_f \neq 1 \\ log_e(2) & for\ A_f = 1 \end{cases} \quad (18.1)$$

$$A_{out} = \frac{A_f}{A_{in}} \quad (18.2)$$

The equations split the total amplification into the two components A_{in} and A_{out} in such a way that the steady-state of the pool is over-estimated for the first half of the time period where the cells stay in the pool and under-estimated for the second half [27].

The ODE system with age classes (ODE AC, Fig. 3C) is similar to the ODE system in Section 2.1.B (ODEs with age classes; Eqs. 2.1–2.2), except that cell numbers are amplified by a factor A_d at every transition between subsequent age classes. Thus, we formulate

$$\frac{dx_1}{dt} = F_{in}(t) - n \cdot k_1 \cdot x_1 \quad (19.1)$$

$$\frac{dx_i}{dt} = n \cdot k_1 \cdot x_{i-1} \cdot A_d - n \cdot k_1 \cdot x_i, \quad i = 2, 3, 4, \ldots n \quad (19.2)$$

$$A_d = \sqrt[n]{A_f} \quad (19.3)$$

$$F_{out} = n \cdot k_1 \cdot x_n \cdot A_d \quad (19.4)$$

For consistency with other models, k_1 is set to 1/τ. Furthermore, the flux leaving the system (Eq. 19.4) is also amplified by A_d, because there are only n–1 transitions between the n age classes, but the cells need to undergo n amplifications of A_d to reach the desired overall amplification of A_f. This requirement of an additional amplification step can be demonstrated by calculating the steady-state values of x_i:

$$\frac{dx_1}{dt}=0 \Rightarrow F_{in}(t)-n\cdot k_1\cdot x_1=0 \Rightarrow x_{1,SS}=\frac{F_{in}}{n\cdot k_1} \quad (20.1)$$

$$\frac{dx_i}{dt}=0 \Rightarrow n\cdot k_1\cdot x_{i-1}\cdot A_d-n\cdot k_1\cdot x_i=0 \Rightarrow x_{i,SS}=x_{i-1,SS}\cdot A_d, \quad i=2,3,4\ldots,n \quad (20.2)$$

Therefore, the steady-state value of the last age class is:

$$x_{n,SS}=x_{n-1,SS}\cdot A_d=\frac{F_{in}}{n\cdot k_1}\cdot (A_d)^{n-1} \quad (20.3)$$

Combining equations Eq. (20.3) and (19.4) shows that we must indeed include the extra amplification A_d. With this inclusion, one obtains

$$F_{out}=n\cdot k_1\cdot\left(\frac{F_{in}}{n\cdot k_1}\cdot (A_d)^{n-1}\right)\cdot A_d=F_{in}\cdot A_f \quad (20.4)$$

Similarly, the discrete system with age classes (DRE, Fig. 3D) can be derived from the DRE in Section 2.1.C if amplification of cells by $A_d=\sqrt[n]{A_f}$ during each transition between age classes is taken into account. This amplification is most easily implemented by substituting the sub-diagonal of ones (Fig 1C, Eq. 4), by a sub-diagonal containing the element A_d.

$$\overrightarrow{X}_{t+1}=V\cdot\overrightarrow{X}_t+\begin{bmatrix}F_{in}(t)\\0\\0\\0\\0\\0\end{bmatrix},\ V=\begin{bmatrix}0&0&0&0&0&0\\A_d&0&0&0&0&0\\0&A_d&0&0&0&0\\0&0&A_d&0&0&0\\0&0&0&A_d&0&0\\0&0&0&0&A_d&0\end{bmatrix} \quad (21)$$

With these definitions both frameworks with age classes, ODE (Eq. 22.1) and DRE (Eq. 22.2), have the same total number of cells over all age classes at their steady-states:

$$X(t)=\sum_i x_i=\frac{F_{in}\cdot(1-A_f)}{1-A_d} \quad (22.1)$$

$$\sum\overrightarrow{X}_\infty=\frac{F_{in}\cdot(1-A_f)}{1-A_d} \quad (22.2)$$

Dynamic responses to an increase in the cell production—Responses of the systems to changes in the cell production were tested by changing F_{in} during the computational experiments. Specifically, we set:

$$F_{in}(t) = \begin{cases} 2 & for\ t \in [0,5] \\ 5 & for\ t \in (5,7] \\ 2 & for\ t \in (7,60] \end{cases} \quad (23)$$

Dynamic responses to a change in the amplification factor—Changes in the amplification factor, A_f, were tested by changing A_f in a time dependent fashion. Specifically, we set:

$$A_f(t) = \begin{cases} 4 & for\ t \in [0,5] \\ 5 & for\ t \in (5,55] \\ 4 & for\ t \in (55,100] \end{cases} \quad (24)$$

Dynamic responses to a change in the rate of differentiation and maturation—To test the responses of the modeling frameworks to dynamic changes in the rate of differentiation and maturation ($1/\tau$), changes to the DRE model must be made, since DRE is the only framework that does not explicitly depend on τ. Even so, the delay is implicitly embedded in the equations, because the number of age classes is determined based on τ and the desired time step, *ts*, which is defined by $n = \tau/ts$.

In order to allow the DRE system to respond to changes of τ, the concept of a relative rate of transition, ν, is proposed. Since τ will change dynamically, the number of age classes needs to be defined relative to a fixed reference τ_{ref}, which corresponds to the length of time it takes for cells to differentiate under normal physiological conditions, so that the number of age classes becomes $n = \tau_{ref}/ts$. The relative rate of transition is therefore defined as $\nu = \tau_{ref}/\tau$. Under physiological conditions, this rate is 1. However, under disease conditions, the relative rate of transition permits the targeted modulation of the rate, with which cells move through the age classes. If τ increases over its reference value, ν becomes smaller than 1, and instead of moving all cells within one age class to the next class, some of the cells are retained in the original age class; that is, they are, in essence, delayed. Analogously, if τ decreases below its reference value, ν becomes larger than 1, and instead of moving all cells in one age class to the next, some of the cells skip a class and move two age classes at once, such that their rate of aging is increased.

To implement this variation in differentiation and maturation rate, three new variables are defined: *r*, the percentage of cells that are retained in the original age class: s_1, the percentage of cells that move to the next age class, and s_2, the percentage of cells that move two age classes. With these settings, we obtain:

$$r(t) = \begin{cases} 1 - v & for\ 0 < v \leq 1 \\ 0 & for\ 1 < v \leq 2 \end{cases} \quad (25.1)$$

$$s_1(t) = \begin{cases} v & for\ 0 < v \leq 1 \\ 2 - v & for\ 1 < v \leq 2 \end{cases} \quad (25.2)$$

$$s_2(t) = \begin{cases} 0\ for\ 0 < v \leq 1 \\ v - 1\ for\ 1 < v \leq 2 \end{cases} \quad (25.3)$$

The explicit formulation of these ratios allows us to adjust the transition matrix of the DRE framework to:

$$V = \begin{bmatrix} r & 0 & 0 & 0 & 0 & 0 \\ s_1 \cdot A_d & r & 0 & 0 & 0 & 0 \\ s_2 \cdot A_d^2 & s_1 \cdot A_d & r & 0 & 0 & 0 \\ 0 & s_2 \cdot A_d^2 & s_1 \cdot A_d & r & 0 & 0 \\ 0 & 0 & s_2 \cdot A_d^2 & s_1 \cdot A_d & r & 0 \\ 0 & 0 & 0 & s_2 \cdot A_d^2 & s_1 \cdot A_d & r \end{bmatrix} \quad (26)$$

With the transition matrix defined as in Eq. (26), cells that remain in the same age class are not being amplified, whereas cells that move two age classes are amplified twice (A_d^2). Consequently, the system settings ensure that the overall amplification factor is retained, independent of the rate of differentiation.

Changes in the rate of differentiation and maturation were tested by changing τ time dependently, and changes in cell production under this new rate of differentiation were tested by changing F_{in}. Thus, we specify:

$$\tau(t) = \begin{cases} 6 & for\ t \in [0, 30] \\ 10 & for\ t \in (30, 225] \\ 6 & for\ t \in (225, 300] \end{cases} \quad (27.1)$$

$$F_{in}(t) = \begin{cases} 2 & for\ t \in [0, 125] \\ 5 & for\ t \in (125, 127] \\ 2 & for\ t \in (127, 300] \end{cases} \quad (27.2)$$

2.4. Comparison with a model from the literature

For further comparisons, we approximated the erythropoietic model developed by Schirm and collaborators [27] with the DRE formalism described in the previous sections, while retaining as much of the original model as possible. In particular, our approximating model includes the same cell types as the original (Fig. 4): erythropoietic stem cells (Stem); burst forming unit-erythroids (BFU-E); colony forming units-erythroids (CFU-E); proliferating erythrocytic blasts (PEB); maturing erythrocytic blasts (MEP); reticulocytes (Reti); and RBCs. To these, we added merozoites (Mer) and infected RBCs (iRBC), which enabled us to model the blood stage of a malaria infection (Fig. 4). Stem and Mer were modeled as single age class pools, whereas all other pools were modeled with a number of age classes,

which was calculated as $n_x=T_x/ts$, where T_x is the normal lifespan of a pool (BFU-E, CFU-E, PEB, MEB, Reti, RBC, iRBC) and *ts* is the duration of the time-step in hours (*cf.* Table 1). In the Schirm model, amplification was approximated by the formalism shown in Figure 3B and Eq. (18), while we modeled it using the formalism shown in Figure 3D, but keeping the parameter values from the Schirm's study. Only the pools BFU-E, CFU-E and PEB were assumed to proliferate. The two RBC pools used in Schirm's model, "random" and "age" were simplified to just one pool, into which all reticulocytes differentiate. As a control, we kept a phantom version of the original random pool and collected in it the number of cells calculated to die; these cells were then removed from the RBC pool by uniformly subtracting cells of all age classes. The pharmacokinetic model of erythropoietin was kept in its original ODE form and used to calculate changes in all of its components from one time point to the next. This was necessary due to the much faster timescale at which the erythropoietin components change relative to the time-scale of cellular differentiation. All other regulatory loops were kept in the same analytical form. Schirm's Chemo-Therapy and Erythropoietin Injection sub-models were omitted as they are not relevant in a malaria infection.

2.5. Model implementation

All models were developed in MATLAB R2014a, using ODE23s and DDE23 functions to solve ODEs and DDEs, respectively, while discrete difference equations were solved recursively with vectorization and a for-loop. The parameter values used were chosen only for illustrative purposes, and do not bear any physical meaning.

3. Results

3.1. Modeling the aging process of infected and non-infected RBCs

The simplest case of modeling RBC dynamics is the normal, healthy situation where RBCs have a fixed lifespan and are constantly generated and randomly removed from the blood stream, for instance, due to wall shear stress; this removal is assumed to occur at any time point with the same low probability. Even this situation is not entirely trivial, because an appropriate model needs to have the ability to account for the more or less fixed delay between the production of a cell and its removal due to old age. This situation may be addressed with delay differential equations (DDEs), ordinary differential equations (ODEs) that approximate DDEs, ODEs with age classes, or discrete recursive equations (DRE) with age classes. We compare these approaches, but do not consider ODEs approximating DDEs, as the two have similar features [10; 28]. In order to allow a fair comparison of the remaining three frameworks, three models were developed (see *Methods*) with internal and external equivalence [26]. Here, internal equivalence refers to the same time delays, while external equivalence requires the same influx and efflux of cells from the system. At steady state, all three models perform similarly, but differences emerge for different scenarios of RBC loss or hormone-controlled changes in RBC production. For illustration purposes, we assume that the lifespan of RBCs is six time units.

Figure 5 shows how each framework responds to a transient increase in the influx of cells. All three systems were initialized at the same steady state with the same numbers of cells

being produced (Fig. 1). At $t = 5$, production was increased for a duration of two time units. As is to be expected, all three systems respond with an increase in the number of cells. Once the production of cells returns to the original value at $t = 7$, the ODE framework immediately starts losing cells, whereas the DDE and the discrete systems maintain the increased number of cells for 6 time units, due to the explicitly specified time delay of 6 time units in the DDE and to the corresponding number of age classes in the DRE framework. At the end of the 6 time units, the DDE and DRE systems return to the original steady-state, which is the expected behavior for RBCs. However, this response is not obtained with an ODE system, even with age classes. The reason can easily be seen in plots B and C of Fig. 5, where the dynamic profile of cells in each age class is shown for the ODE (Fig. 5B) and discrete (Fig. 5C) systems. In the discrete system, the increased number of cells is retained for two time units in each age class, before the cells are transferred to the next class. Once the last age class is reached, the increased number of cells leaves the system, which thereby returns to the original steady-state. The ODE system responds very differently. As soon as the number of cells increases in the first age class, some cells start moving throughout the following age classes, with some cells starting to leave the system almost immediately. Within 6 time units, the system is already half way back to the original steady state, while the remaining cells leave the system at a progressively slower rate (Fig. 5B), and the steady state is mathematically only reached for $t \to \infty$. These results highlight the challenges encountered when an ODE framework is used to address the RBC aging process.

3.2. Modeling the premature removal of infected and non-infected RBCs

At any time point in their life cycle, infected and non-infected RBCs may be removed by age-independent processes. For instance, non-infected RBCs may be infected or lysed due to shear-stress between the blood stream and the vessel wall, and infected RBCs may be destroyed by the immune system. An effective model must be able to capture these processes appropriately. Thus, we simulated the removal of cells in the same modeling frameworks as before; the results are shown in Figure 6. The removal causes the ODE and DRE systems to move to a lower steady-state (Fig. 6A). When the cell production is subsequently increased (at $t = 5$), these two models exhibit a similar behavior as was observed before (Fig. 5A), except for the fact the number of cells in the discrete system declines (between t=7 and t=13) due to the removal of cells from all age classes. *A priori* surprisingly, the DDE model behaves quite differently, and the cell population plummets. The reason is that some of the same cells are incorrectly removed twice. The first removal occurs through natural cell death, which is modeled through the removal of as many cells at time t as had entered the system at time $t - \tau$, where τ is the lifespan of an RBC (see *Methods* section). In addition, the age-independent process removes some of these cells again. The result is a strong decline in the RBC population in the DDE model (Fig. 6A). As discussed in the *Methods* section, it is possible to correct for this double-counting, when the original DDE (Eq. 7.1) is replaced by Eq. (7.3), which adds back the doubly counted cell loss in an averaged manner. With this correction, the DDE behavior is not identical to the DRE model, but much closer. One might also mention that the correction in Eq. (7.1) requires that the term for the age-independent cell removal can be analytically integrated, which might not be the case for other blood loss scenarios. A numerical integration of the

removal flux would also allow for a correction of the DDE function, but additional equations would have to be used. Panels 6B and 6C show the dynamics of cell sub-populations in the six age classes.

The framework that best captures the behavior of RBC aging with or without extra removal processes is the discrete recursive framework with age classes. ODE models with or without age classes produce responses that are in a sense averaged and thereby represent age-independent perturbations or interventions as rather coarse approximations.

3.3. Modeling RBC progenitor and precursor cells

The combined differentiation and maturation process of progenitor and precursor cells is dynamically different from RBC aging, because the organism has the capacity to adjust the rates of these processes in response to stresses, whereas RBC aging is a somewhat passive, predetermined process. Moreover, differentiation leads to a progressive expansion of the number of cells, so that the number of cells that enter a pool at a given time is much smaller than the corresponding number of cells that leave the same pool fully differentiated. This increase constitutes the amplification factor of a given pool, and it too changes dynamically in response to cytokines like erythropoietin if more RBCs are needed.

Four modeling frameworks (see *Methods*) are compared with respect to their ability to capture the dynamics of cell differentiation and maturation: A) an ODE system with an expansion process but without age classes (ODE IA); B) an ODE system without age classes where the population expands when cells enter and leave a pool (ODE EA); C) an ODE system with age classes where amplification occurs during the transition between age classes (ODE AC); and D) a DRE system with age classes and with amplification during the transition between age classes (see *Methods* for details).

The four frameworks were set up while ensuring external and internal equivalence. Here, internal equivalence mandates the same or a similar steady-state number of cells, delay, number of age classes, and rate of differentiation and maturation, while external equivalence is given by the same amplification factor and the same number of cells entering and leaving the system at steady state.

Although the systems were made as similar to each other as possible, the ODE systems without age classes cannot attain the same steady-state value as the other two systems (Fig. 7A). The reason is that it is mathematically not possible to obtain the same throughput as well as the same baseline steady state in this type of expanding system. Specifically, due to the features of the population growth process (see *Methods* section), the steady state for the ODE system with internal growth is $X_{SS} = F_{in} \cdot A_f \cdot \tau$ (Eq. 13.3) whereas it is $\Sigma X_{\infty} = F_{in} \cdot (1 - A_f) \cdot (1 - A_d)^{-1}$ (Eq. 22.2) for the discrete system (see Section 2.3). The combination of the much higher steady-state value and the two first-order processes of population growth and cell removal leads to the low turn-over of this ODE system, which causes it to respond much more slowly than the other frameworks. Due to this behavior, this framework will not be discussed further. The ODE with amplification before entering and after leaving a pool also has a different steady-state than the frameworks with age classes, but this difference is

dependent on the actual definition of A_{in} and A_{out}. We defined these as proposed by Schirm *et al.* [27] and shown in Eqs. (18.1–18.2) of the *Methods* Section 2.3.

When the four systems were tested for their dynamic response to an increase in the cell production (Fig. 7), all had similar dynamics except for the ODE system with internal growth (ODE IA). Its steady-state is higher and the dynamical behavior is slower than the other two ODE frameworks. Both frameworks with age classes (DRE and ODE AC) behave similarly, whereas the discrete system (DRE) exhibits the most rigid temporal behavior. In comparison with the results shown in Figs. 5 B and C, each age class of the DRE model now contains a different number of cells, which is due to the amplification factor $\left(A_d = \sqrt[n]{A_f}\right)$ with which the cell population expands every time the cells move from one age class to the next. The particular amplification factor ensures that the total population expands by a total of A_f by the end of the n^{th} age class.

Considering that these model frameworks need to allow dynamic changes in the value of the amplification factor, the response to such a change was investigated (Fig. 8). As expected, an increased amplification factor leads to an increase in the steady-state, as well as an increased output of cells from the systems under the new steady state. The two systems with age classes show a faster change in steady-state than the ODE without age classes. The discrete system responds with a crisper profile, whereas the ODE system with age classes exhibits smother transitions between steady-states. Nevertheless, both systems with age classes have a very similar response profile.

Similarly, the response to a change in the rate of differentiation and maturation was investigated. Moving cells faster (or more slowly) through a constant number of age classes is easily implemented in an ODE framework, since the first-order rate of cell aging from one age class to the next explicitly includes the average overall time it will take a cell to move through all the age classes. This rate for each age class is n/τ, where n is the number of age classes and τ is the differentiation time. Thus, a dynamical change in τ "automatically" produces the desired effect. The same concept of an increased rate can be approximated in the discrete system. Namely, instead of moving all cells of a given age class to the next class in one time-step, only a portion of the cells moves to the next age class, while the remaining cells either move two age classes or remain in the original age class, depending on whether the rate of differentiation is increased or decreased, respectively. In other words, instead of defining the recursive process through a transition matrix with values only in the sub-diagonal, as it is found in a typical shift matrix, values (different from zero) may also be present in either the sub-sub-diagonal or in the diagonal, depending on the direction of the change (see *Methods* Section, Eq. 26).

As before, the behavior of the alternative frameworks was tested with respect to a change in differentiation rate. Fig. 9 shows the response of each system towards a decrease in the rate of differentiation (at $t = 25$), followed by an increase in the number of cells entering the pools at $t = 125$, for two time units; at $t = 225$ the differentiation rate was returned to its original value. As soon as the rate of differentiation is decreased, all three systems react with a similar increase in steady state. As in the previous case, the two systems with age classes

present the same initial and final steady states, whereas the ODE without age classes exhibits lower steady states. Closer examination of the behavior of the age classes (Fig. 9 B, C) reveals that the profiles of the continuous and the discrete systems are almost identical in this case. The reason is that the transitions between age classes in the discrete system become “probabilistic" under a lower rate of differentiation, so that only a percentage of the cells moves to the next age class and the remaining cells stay in the original age class. This process resembles how a first-order term moves cells from one age class to the next in the continuous system. When the number of cells entering the system is increased, the responses of these two systems are qualitatively similar and differ only slightly quantitatively. The two systems show the typical qualitative difference as soon as the rate of differentiation is brought back to the original value. At this point all cells in the age classes of the discrete system move to the next age class at every time step and the system shows the crisp temporal behavior that it exhibited in the previous cases.

3.4. Modeling erythropoiesis during a malaria blood stage infection

Given that the discrete framework with age classes performs equally well or better than other alternatives under all representative perturbations tested, we chose this framework to develop an illustration model of the malaria blood stage infection and erythropoiesis. For the RBC precursor system, we approximated the model developed by Schirm and collaborators [27] for the erythropoietic response in humans to erythropoietin and chemotherapy. For the blood stage of malaria, we approximated a Lotka-Volterra model in a discrete manner. The overall model scheme is shown in Figure 10. All cells were modeled with age classes except for the multipotent stem cells (Stem) and the merozoites (Mer). These were assumed to be single age class pools. A pharmacokinetic model of erythropoietin was incorporated from Schirm’s model as an ODE module. The number of age classes for each cell type was determined as the closest integer of the ratio between the differentiation, maturation or lifespan time under normal (healthy) steady-state condition and the time step length of the simulation (Table 1). The pools of BFU-E, CFU-E, PEB and MEB respond to erythropoietin with a changed speed of differentiation and maturation [27], and BFU-E, CFU-E and PEB also respond by changing the amplification factor [27]. Changes in the differentiation and maturation speed were implemented as shown above (Section 2.3., Eqs. 26 and 27), but by setting the transition time to $\nu = n \cdot ts/\tau$, where n is the number of age classes, ts the time step duration and τ the dynamical lifespan or differentiation time of the cell pool. Given that the number of age classes is defined by the normal differentiation time and the length of the time step, the percent change in the time of differentiation is used to change the rate of movement of cells through the different age classes. Specifically, if the differentiation time decreases below the control value, the rate of cell progression through the age classes is increased by the same amount. The lifespan of iRBC can be changed from 24 to 72 hours depending on the species of *Plasmodium* being simulated.

Figure 11 shows the result of a simulation of the erythropoietic response to a malaria infection starting at day 5 with 1 merozoite per 10 million RBCs and cured by chemical intervention at day 20. Progress of the infection (iRBCs and merozoites) is shown in Figure 12. Destruction of RBCs by the parasite results in anemia, which causes an up-regulation of erythropoiesis (Fig. 11). By keeping the original parameters [27], the our model predicts the

same fluxes, but since all cellular pools have age classes, instead of a single ODE, the concentrations are not numerically the same as the original model. Just like in the examples in Figures 7, 8 and 9, the DRE model always has a higher numbers of cells (under steady state and during dynamic shifts) than the ODE framework with external amplification (ODE EA). The same does not occur at the level of RBCs, as both frameworks predict the same amount of cells for the same influx of cells (as is the case of Fig. 5: compare DRE and ODE). The strength of the bone marrow inhibitory loop on the differentiation of stem cells had to be decreased because of the strict imposition of the delays in this DRE model. In our DRE model, the full strength of the inhibitory loop creates an oscillatory response to anemia, since anemia causes an higher production rate of RBC precursors, which leads to an increased number of bone marrow cells which, in turn, decreases the magnitude of stem cell differentiation, once the amount of precursors decreases; while anemia remains unresolved, stem cell differentiation increases, and the cycle starts over again. A proper way to resolve these issues could be to re-parameterize this DRE model using the same experimental data used to parameterize Schirm's model [27], but because the example only serves as illustration, such a re-parameterization seems unnecessary.

4. Discussion

Developing a model for erythropoiesis and RBC dynamics that reproduces observations with reasonable accuracy requires a modeling framework capable of keeping cells in various pools for more or less fixed periods of time after their generation. One approach toward such a model is to define a delay characterizing the entry and exit from these pools. At first, the framework of choice appears to be a delay differential equation (DDE) model. Indeed, such a model works well if the production and degradation are the only significant processes in the system (Fig. 5, panel A). However, if other processes need to be captured, such as the ability to remove cells from a pool in a singular discrete event, the DDE formulation becomes cumbersome. For instance, the capacity to include additional processes requires that these processes can be integrated, so that the number of cells lost by the secondary processes is not counted twice and may be removed from the delay degradation term. Also, the initial state of the system in a DDE model is actually independent of the influxes and effluxes, which is counterintuitive when, for instance, the model is supposed to capture the lifespan of RBC (see Figs. 5A and 1a). As a specific example, humans have approximately 5 million RBCs per μL of blood [25], and RBCs live on average 120 days [25], so that the daily production of RBCs is about 42,000 RBCs/day/μL of blood. Intuitively, if the production rate changes, the number of RBCs should change, accordingly. However, in a DDE model as shown in Figure 1i (Eq. 1.2) the initial number of RBCs at t=0 and the influx $F_{in}(t)$ are actually disconnected, and the system can be initialized with different settings, yet remain at the same start value as long as $F_{in}(t)$ does not change. Thus, the DDE model response does not accurately reflect the natural behavior of the biological system.

Delays can also be approximated with ODEs, but a single ODE cannot produce an output as the one generated by the DRE or the DDE models in Fig. 5. Some mathematical reformulations may produce better approximations, like the ODEs with internal and external amplification whose output was shown in Figures 7, 3A, and 3B, but these will still not produce that crisp delay observed in Fig. 5. Indeed, not even the addition of age classes

produces a truly crisp delay. It may be argued that an ODE framework with a sufficiently high number of age classes would produce an output that would closely approximate the results in of the DRE and DDE in Fig. 5. While this assessment is true, this strategy would require a very large number of age classes, which would make the ODE system expensive in terms of both required memory and computational time. PDEs could be used to remedy these challenges, but they are mathematically rather inflexible with respect to discrete events affecting the system. They were therefore not used in this work.

By contrast, DREs with age classes are as easy to use as ODEs, while at the same time permitting matrix formulations that are very compact and effective. Given that the number of age classes is dependent on the size of the time-step, choosing overly small time-steps leads to large numbers of age classes that may consume memory and processing time. However, there are various solutions that can mitigate this issue. First, the calculations may be done with a small time step but not all time steps are recorded. Secondly, for large systems, a huge, although sparse, transition matrix may not be the best solution. Instead, it may be advantageous in these cases to move cells in each pool recursively. Specifically, auxiliary variables may be used to keep record of each pool X and its position in the main $X_i(t)$ vector (*e.g.*, poolX=123:245). With such a setting, all cells in poolX may be moved independently of the number of age classes in pool X, according to the pseudo-code below:

Let A= $X_i(t+1)$ and B= $X_i(t)$

A=B*0 (*A* is initiated as a vector of zeros with the same size as *B*)

A(poolX+1)=B(poolX)

The cells that have left pool X at $t+1$ are removed from the extra age class by setting: poolX_out=A(poolX(end)+1) and A(poolX(end)+1)=0.

The cells that came from pool IX (poolIX_out) may then be added to the first age class of pool X:

A(poolX(1))= poolIX_out

With this type of coding, the representation of the DRE system is independent of the number of age classes attributed to each pool, as long as that information exists in auxiliary variables. Also, a few extra age classes may have to be reserved at the end of each pool to receive cells leaving each pool. An equivalent formulation would be difficult to implement with a transition matrix, as a new matrix would have to be calculated for each new set of numbers of age classes in each pool.

DREs as shown here represent the passage of time better than ODE systems.

Acknowledgments

The authors would like to thank Po-Wei Chen, James Wade, Daniel Olivença, Sepideh Dolatshahi and Mojdeh Faraji for helpful comments and discussions. This project was funded in part by Federal funds from the US National Institute of Allergy and Infectious Diseases, National Institutes of Health, Department of Health and Human Services under contract # HHSN272201200031C, which supports the Malaria Host–Pathogen Interaction Center (MaHPIC).

References

1. WHO. World Malaria Report 2013. 2013
2. Mangano VD, Modiano D. An evolutionary perspective of how infection drives human genome diversity: the case of malaria. Curr Opin Immunol. 2014; 30C:39–47. [PubMed: 24996199]
3. Taylor SM, Cerami C, Fairhurst RM. Hemoglobinopathies: slicing the Gordian knot of *Plasmodium falciparum* malaria pathogenesis. PLoS Pathog. 2013; 9:e1003327. [PubMed: 23696730]
4. Nagel RL, Roth EF Jr. Malaria and red cell genetic defects. Blood. 1989; 74:1213–21. [PubMed: 2669996]
5. Miller LH, Ackerman HC, Su XZ, Wellems TE. Malaria biology and disease pathogenesis: insights for new treatments. Nat Med. 2013; 19:156–67. [PubMed: 23389616]
6. Weatherall DJ, Miller LH, Baruch DI, Marsh K, Doumbo OK, Casals-Pascual C, Roberts DJ. Malaria and the red cell. Hematology Am Soc Hematol Educ Program. 2002:35–57. [PubMed: 12446418]
7. Moreno A, Cabrera-Mora M, Garcia A, Orkin J, Strobert E, Barnwell JW, Galinski MR. Plasmodium coatneyi in rhesus macaques replicates the multisystemic dysfunction of severe malaria in humans. Infection and Immunity. 2013; 81:1889–904. [PubMed: 23509137]
8. Perkins DJ, Were T, Davenport GC, Kempaiah P, Hittner JB, Ong'echa JM. Severe malarial anemia: innate immunity and pathogenesis. Int J Biol Sci. 2011; 7:1427–42. [PubMed: 22110393]
9. Douglas NM, Anstey NM, Buffet PA, Poespoprodjo JR, Yeo TW, White NJ, Price RN. The anaemia of Plasmodium vivax malaria. Malar J. 2012; 11:135. [PubMed: 22540175]
10. Mocek WT, Rudnicki R, Voit EO. Approximation of delays in biochemical systems. Math Biosci. 2005; 198:190–216. [PubMed: 16181644]
11. Wu J, Qi Z, Voit EO. Impact of delays and noise on dopamine signal transduction. In Silico Biol. 2010; 10:67–80. [PubMed: 22430222]
12. Kerlin DH, Gatton ML. Preferential invasion by *Plasmodium* merozoites and the self-regulation of parasite burden. PLoS One. 2013; 8:e57434. [PubMed: 23460855]
13. Manesso E, Teles J, Bryder D, Peterson C. Dynamical modelling of haematopoiesis: an integrated view over the system in homeostasis and under perturbation. J R Soc Interface. 2013; 10:20120817. [PubMed: 23256190]
14. Johnson PLF, Kochin BF, Ahmed R, Antia R. How do antigenically varying pathogens avoid cross-reactive responses to invariant antigens? Proceedings of the Royal Society B-Biological Sciences. 2012; 279:2777–2785.
15. Scholz M, Gross A, Loeffler M. A biomathematical model of human thrombopoiesis under chemotherapy. Journal of Theoretical Biology. 2010; 264:287–300. [PubMed: 20083124]
16. McQueen PG, McKenzie FE. Age-structured red blood cell susceptibility and the dynamics of malaria infections. Proceedings of the National Academy of Sciences of the United States of America. 2004; 101:9161–9166. [PubMed: 15178766]
17. Bocharov GA, Rihan FA. Numerical modelling in biosciences using delay differential equations. J Comput Appl Math. 2000; 125:183–199.
18. Greischar MA, Read AF, Bjornstad ON. Synchrony in malaria infections: how intensifying within-host competition can be adaptive. Am Nat. 2014; 183:E36–49. [PubMed: 24464205]
19. Loeffler M, Pantel K, Wulff H, Wichmann HE. A Mathematical-Model of Erythropoiesis in Mice and Rats. 1. Structure of the Model. Cell and Tissue Kinetics. 1989; 22:13–30. [PubMed: 2790923]
20. Hosseini SM, Feng JJ. How malaria parasites reduce the deformability of infected red blood cells. Biophys J. 2012; 103:1–10. [PubMed: 22828326]
21. Tumwiine J, Luckhaus S, Mugisha JYT, Luboobi LS. An Age-structured Mathematical Model for the Within Host Dynamics of Malaria and the Immune System. Journal of Mathematical Modelling and Algorithms. 2008; 7:79–97.
22. Belair J, Mackey MC, Mahaffy JM. Age-structured and two-delay models for erythropoiesis. Math Biosci. 1995; 128:317–46. [PubMed: 7606142]

23. McKenzie FE, Bossert WH. An integrated model of *Plasmodium falciparum* dynamics. J Theor Biol. 2005; 232:411–26. [PubMed: 15572065]
24. Kaushansky, K.; Lichtman, M.; Beutler, E.; Kipps, T.; Prchal, J.; Seligsohn, U. Williams Hematology. Eighth. McGraw-Hill Education; 2010.
25. Sherwood, L. Human physiology from cells to systems. Belmont, CA: Wadsworth Pub. Co; 1997.
26. Savageau MA. A theory of alternative designs for biochemical control systems. Biomed Biochim Acta. 1985; 44:875–80. [PubMed: 4038287]
27. Schirm S, Engel C, Loeffler M, Scholz M. A biomathematical model of human erythropoiesis under erythropoietin and chemotherapy administration. PLoS One. 2013; 8:e65630. [PubMed: 23755260]
28. Wu J, Voit E. Hybrid modeling in biochemical systems theory by means of functional petri nets. J Bioinform Comput Biol. 2009; 7:107–34. [PubMed: 19226663]
29. Gutierrez JB, Galinski M, Cantrell S, Voit EO. From Within Host Dynamics to the Epidemiology of Infectious Disease: Scientific Overview and Challenges. Math Biosc. in press.
30. Voit, EO. A First Course in Systems Biology. Garland Science; New York, NY: 2012. p. xiv-445.

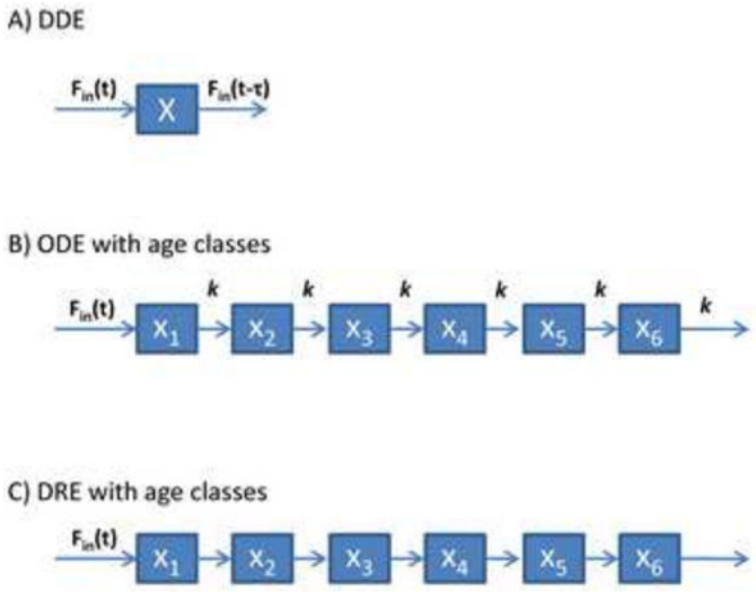

Fig. 1.

Conceptual schemes for the different modeling frameworks used to investigate the aging process of uninfected red blood cells (RBCs) and infected RBCs (iRBCs). Three frameworks were set up to model cells with fixed lifespan: A) DDE, B) ODE with age classes, and C) DRE with age classes. In A) a single pool is considered with $F_{in}(t)$ cells entering and $F_{in}(t-\tau)$ exiting the pool after a delay of 6 time units (τ=6). In B) $F_{in}(t)$ cells enter a system with a single pool of n=6 age classes, which approximates a delay τ of 6 time units; transitions between age classes have a rate of $k=n/\tau$. In C), a single pool with age classes is modeled with discrete recursive equations.

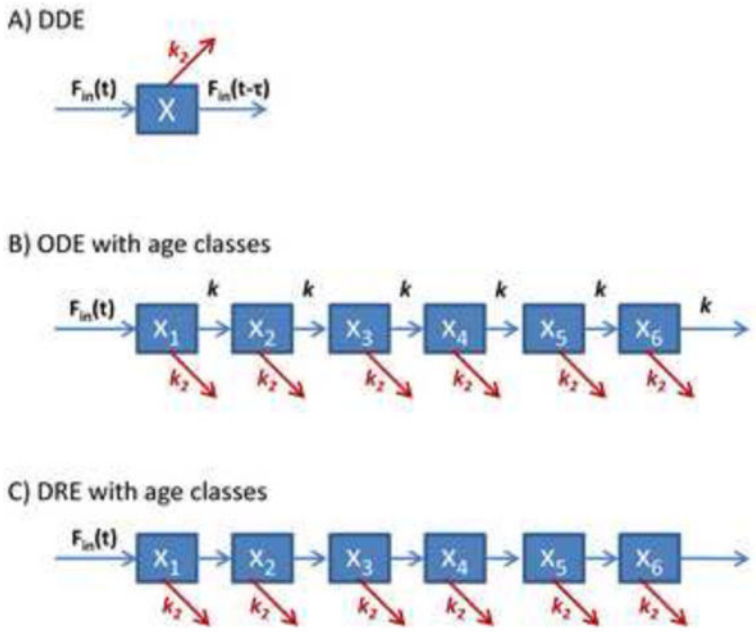

Fig. 2.

Conceptual schemes for the three frameworks used to model the aging process of RBCs and iRBCs with an additional age-independent flux of cell removal. Three frameworks were set up to model cells with a fixed lifespan. Cells are either removed by an age-independent flux, modeled as a first-order process with a rate constant k_2=1/12, or at the end of their lifespan. In A) the age-independent removal process is simply added to the DDE formulation; this procedure results in the dual removal of some cells, which has to be corrected (see Eq. (7.1–7.3) in the *Methods* section). In B) and C), the age-independent removal process is added to all age classes.

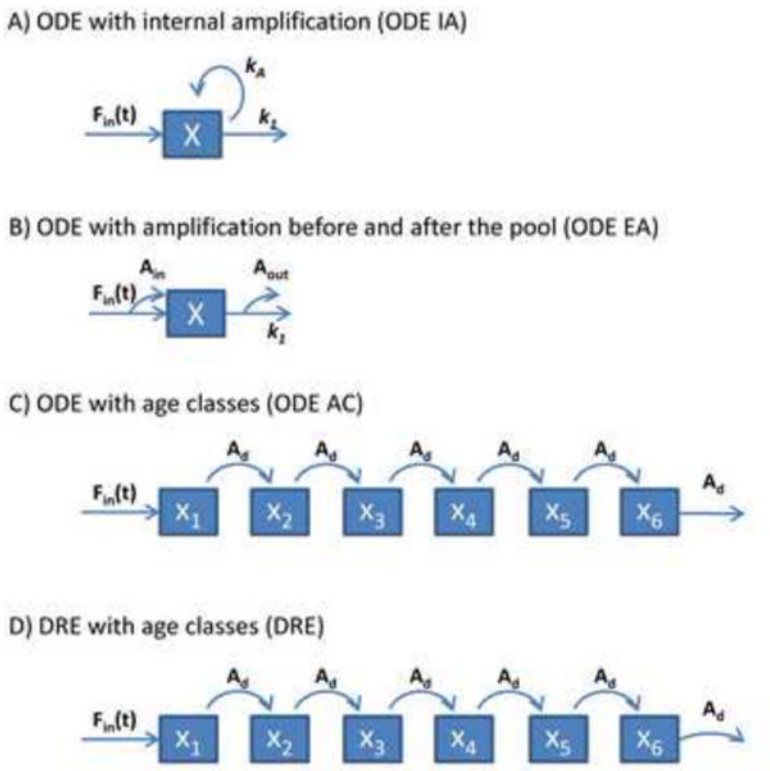

Fig. 3.

Schemes for different frameworks used to model the differentiation process of cells with variable lifespans and amplification factors, as they are encountered in erythroid progenitor or precursor cells. Four frameworks were set up. In A), a single pool is modeled using ODEs where $F_{in}(t)$ cells enter and $F_{out}(t)$ cells leave the pool, such that the amplification factor is $A_f = F_{out}/F_{in}$. Correspondingly, the growth rate k_A under steady-state conditions was defined as $k_1 - k_1/A_f$. In B), a single pool with partial amplification A_{in} for entering cells and A_{out} for exiting cells was modeled with an ODE, such that $A_f = A_{in} \cdot A_{out}$. In C), a single pool with age classes is modeled using ODEs with partial-amplification $A_d = \sqrt[n]{A}$ during transitions between age classes. In D), a single pool with age classes is modeled using DREs with partial amplification events ($A_d = \sqrt[n]{A}$) between age classes. See Text for the expansion of the model in D) to account for a variable lifespan.

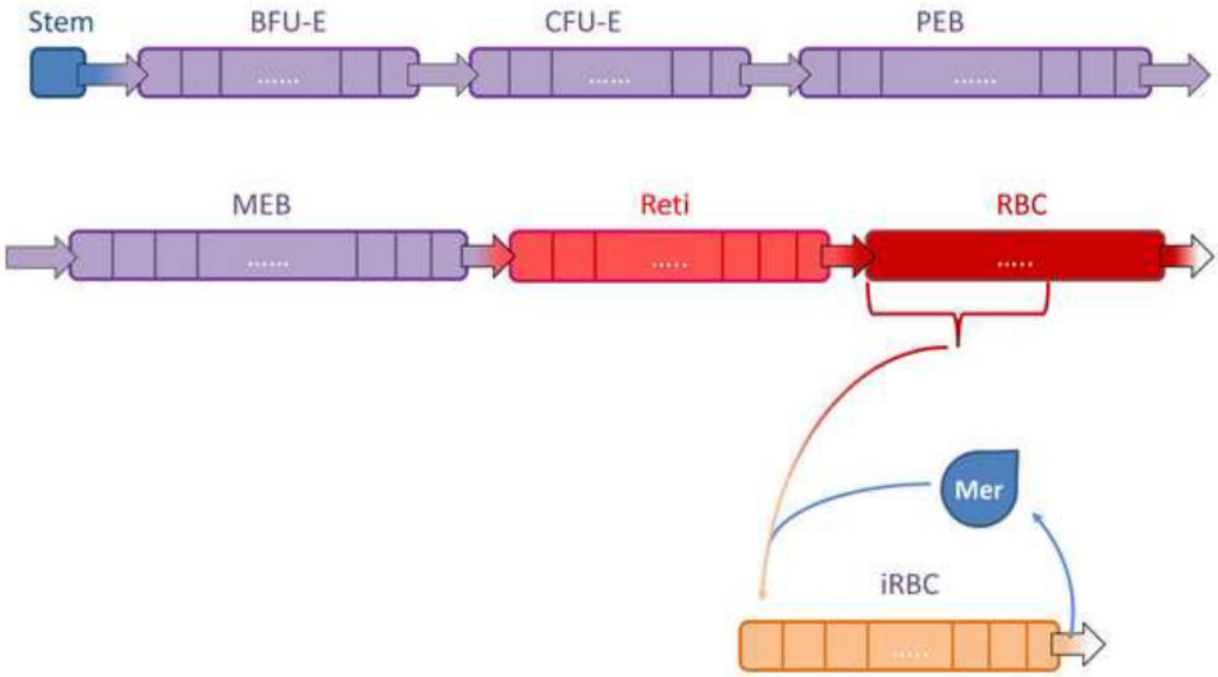

Fig. 4.

Scheme of a DRE model with age classes for erythropoiesis and blood-stage malaria infection that corresponds to Schirm's erythropoietic model [27]. The malaria blood-stage infection is modeled using a Lotka-Volterra model. The various cellular pools are allowed to have different numbers of age classes ($n_x=T_x/ts$), which reflect the duration of the time-step (ts) and the lifespan of the particular cell pool (T_x). Only stem cells and merozoites (Mer) are assumed to have one age class. See Table 1 for numbers of age classes. The bracket under the RBC pool indicates age class preferences of different malaria parasite species.

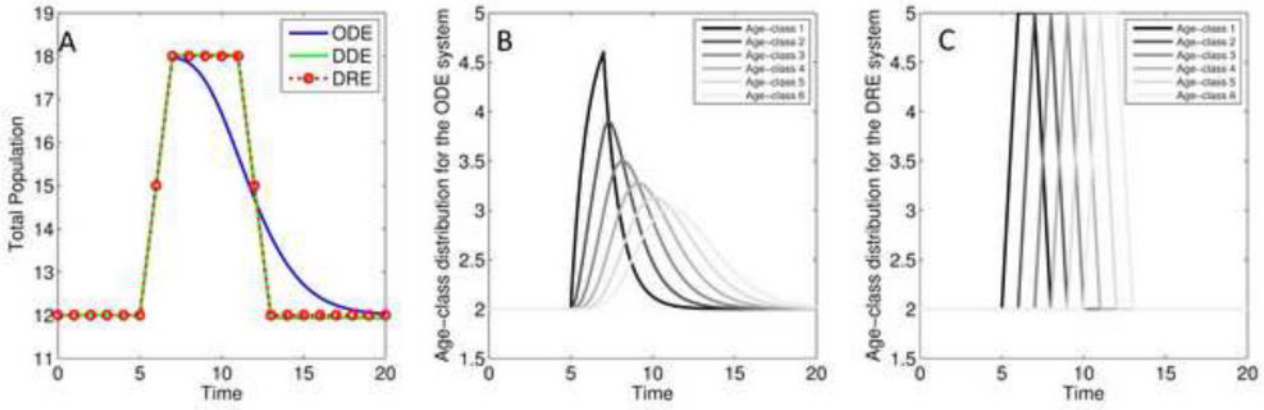

Fig. 5.

Comparison of the dynamical responses to a transient increase in cell influx by three different frameworks capable of modeling cells with fixed lifespan: ODE with age classes (ODE; ——); DDE (DDE; ——); and discrete recursive equation (DRE; ·-●-·) with age classes. The models were set up with as much internal and external equivalence as possible (see Text). Panel A shows the simulation results for the total numbers of cells for the three frameworks. Panels B and C present the numbers of cells obtained for each age class of the ODE and DRE frameworks, respectively. These are shown with a color gradient from black (first age class) to light gray (sixth age class). The DDE and DRE frameworks behave equally well, as additional cells enter the pools between $5 < t \leq 7$. These cells are assumed to remain in the pool for $\tau = 6$ time units. Thus, τ is the value of the delay in the DDE and also the number of age classes in the DRE and ODE frameworks. The ODE does not capture the sustained increase in cell number and instead immediately starts losing cells.

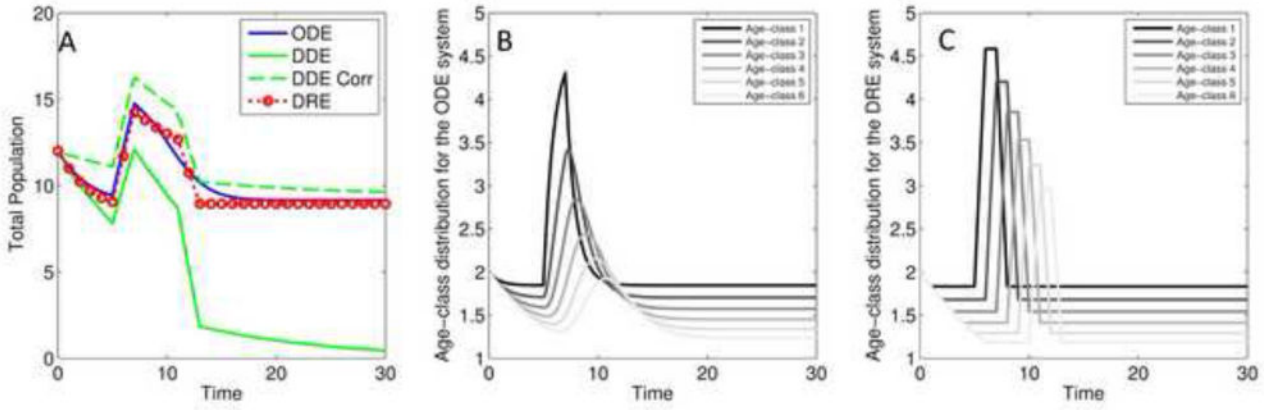

Fig. 6.

Comparison of the dynamical responses to a transient increase in cell influx by three different frameworks that are capable of modeling cells with fixed lifespan and furthermore allow continuous random loss: ODE with age classes (ODE; ——); DDE (DDE; —— and DDE corr; – – –); and discrete recursive equation (DRE; ·-●-·) with age classes. All models were set up with as much equivalence as possible (see Text). Panel A shows the simulation results for the total numbers of cells for the four frameworks. Panels B and C show the numbers of cells in each age class of the ODE and DRE frameworks, respectively. These are shown with a color gradient from black (first age class) to light gray (sixth age class). The addition of a first-order term for cell removal to the DDE (DDE; ——) does not accurately represent the system (Eq. 7.1), but a correction (Eq. 7.3) remedies the performance to some degree (DDE corr; – – –). Once corrected, the DDE framework (DDE Corr) performs similarly to the DRE, although it takes a very long time for the system to reach the steady-state, whereas the other two frameworks reach their steady states more quickly. Similar to the previous study without a random process of cell removal (Fig. 5), the ODE framework with age classes does not retain the extra number of cells that enter the pool between $5 < t \leq 7$ for the expected 6 time units. Overall, the DRE system emerges as the preferred option for modeling a cell population with a fixed lifespan that is furthermore subject to random, age-independent, losses.

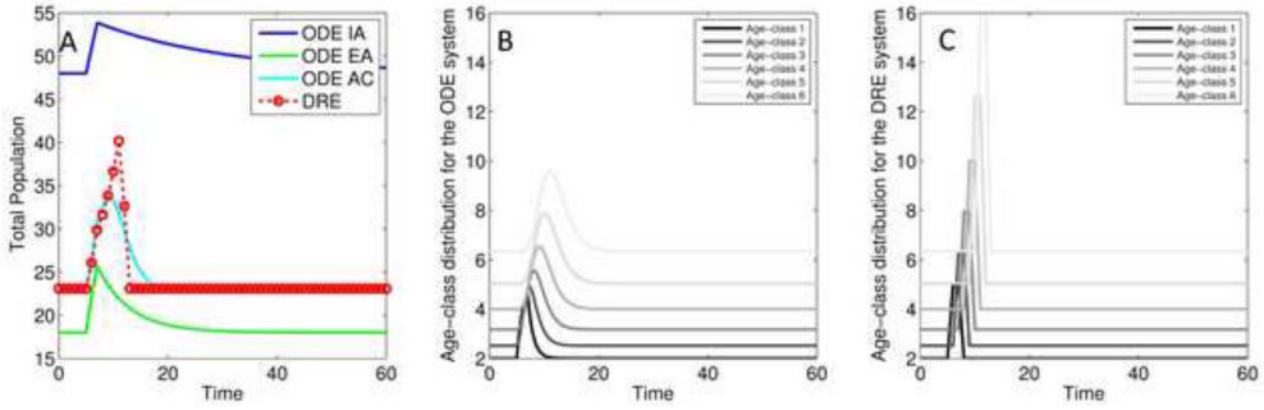

Fig. 7.

Comparison of the dynamical responses to a transient increase in cell influx by four different frameworks capable of modeling cells with variable lifespan and amplification factor: ODE with internal amplification (ODE IA; ——); ODE with external amplification (ODE EA; ——); ODE with age classes (ODE AC; ——); and discrete recursive equation (DRE; ··●··) with age classes. All models were set up with as much equivalence as possible. Panel A shows the simulation results for the total numbers of cells for all frameworks. Panels B and C show the numbers of cells in each age class of the ODE and DRE frameworks, respectively. The results are shown with a color gradient from black (first age class) to light gray (sixth age class). Only the frameworks with age classes perform reasonably well, and of these the best is DRE, as it retains the crisp temporal behavior that is expected from the biology of the system.

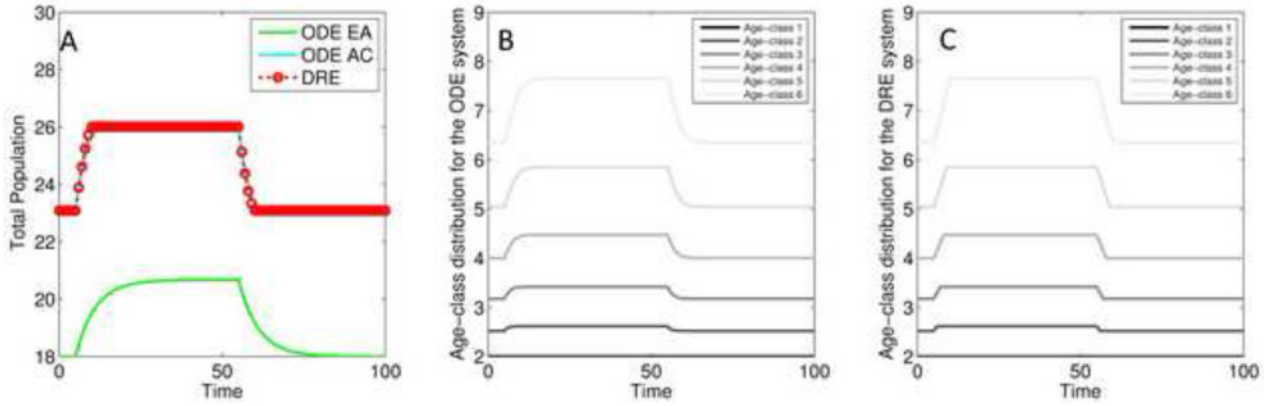

Fig. 8.

Comparison of the dynamical responses to a transient increase in the amplification factor by three different frameworks capable of modeling cells with variable lifespans and amplification factor: ODE with external amplification (ODE EA; ——); ODE with age classes (ODE AC; ——); and discrete recursive equation (DRE; -·-·-) with age classes. All models were set up with as much equivalence as possible (see Text). Panel A shows the simulation results for the total numbers of cells for all frameworks. Panels B and C show the numbers of cells in each age class of the ODE and DRE frameworks, respectively. These are shown with a color gradient from black (first age class) to light gray (sixth age class). The frameworks with age classes performed very similarly to each other, while the ODE with external amplification is a reasonably good approximation of the frameworks with age classes, considering that this framework consists of only one differential equation.

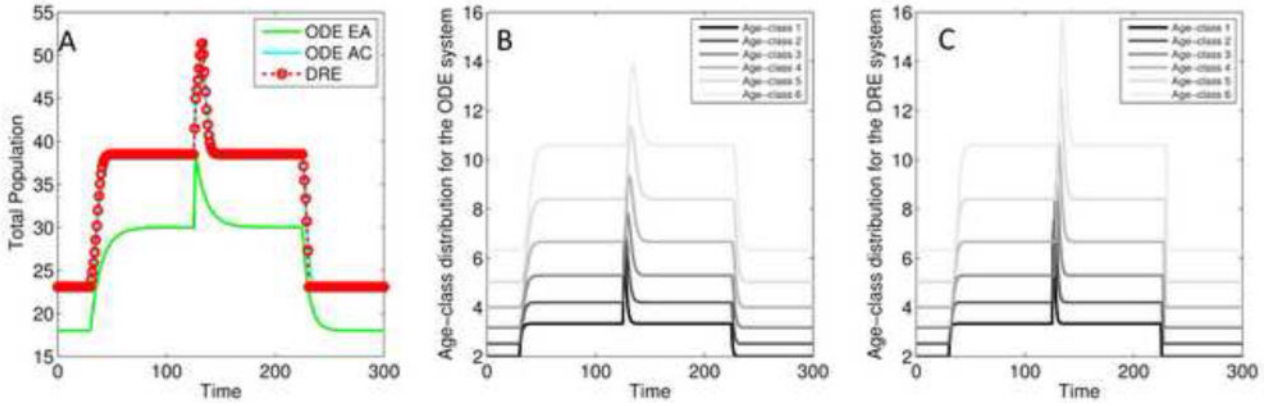

Fig. 9.

Comparison of the dynamical responses to a transient increase in lifespan by three different frameworks capable of modeling cells with variable lifespans and amplification factors: ODE with external amplification (ODE EA; ——); ODE with age classes (ODE AC; ——); and discrete recursive equation (DRE; ·-●-·) with age classes. All models were set up with as much equivalence as possible (see Text). Panel A shows the simulation results for the total numbers of cells for all frameworks. Panels B and C show the numbers of cells in each age class of the ODE and DRE frameworks, respectively. These are shown with a color gradient from black (first age class) to light gray (sixth age class). Changing the rate of differentiation causes the DRE framework to lose its temporal crispness and behave similarly to the ODE with age classes (Fig. 7 B, C), as can be seen in the response to a change in the cell influx during the time period $125 < t \leq 127$.

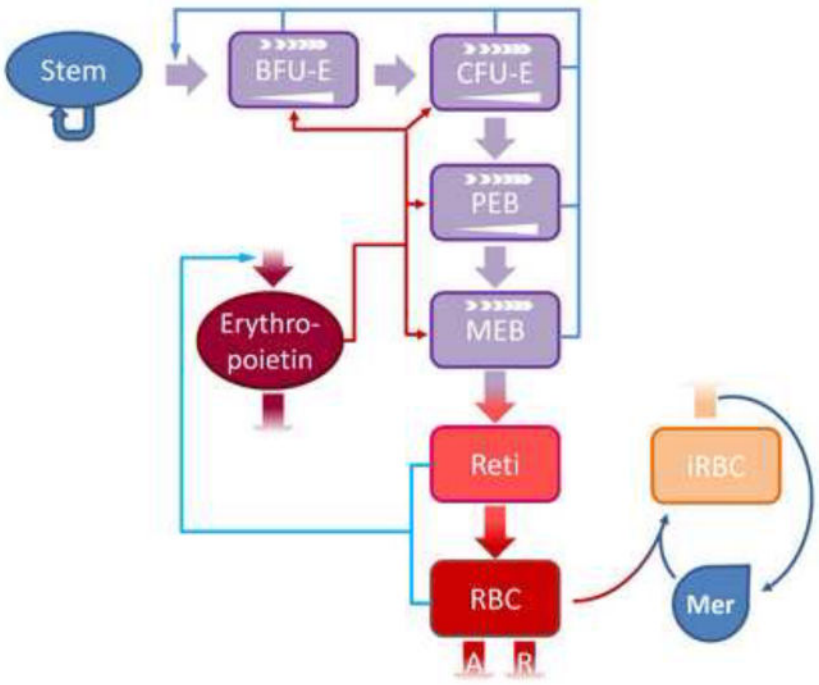

Fig. 10.

Scheme of a DRE model with age classes for erythropoiesis and blood-stage malaria infection that corresponds to Schirm's erythropoietic model [27]. The malaria blood-stage infection is modeled with a Lotka-Volterra model. In this model, stem cells (Stem) constitute a self-sustained pool that also generates burst forming unit-erythroids (BFU-E). These differentiate sequentially into colony forming unit-erythroids (CFU-E), proliferating erythrocytic blasts (PEB) and maturing erythrocytic blasts (MEP). MEP give rise to circulating reticulocytes (Reti), which finally differentiate into circulating RBCs. Erythropoiesis is modeled with three regulatory loops. RBCs and reticulocytes transport oxygen, which negatively regulates the production of erythropoietin (shown in green). Erythropoietin also regulates the amplification ( ) of BFU-E, CFU-E and PEB and the rate of differentiation ( ) of BFU-E, CFU-E, PEB and MEB (shown in scarlet thin arrows); in turn, the number of progenitor and precursor cells in the bone marrow negatively regulates the number of stem cells (shown in turquoise). RBCs are subject to random, age-independent loss (R), in addition to the natural age-dependent loss (A) at the end of their lifespan. When present, merozoites (Mer) can infect RBCs of certain age classes. At the end of their lifespan, the infected RBCs (iRBC) burst, giving rise to 8–32 new merozoites per iRBC.

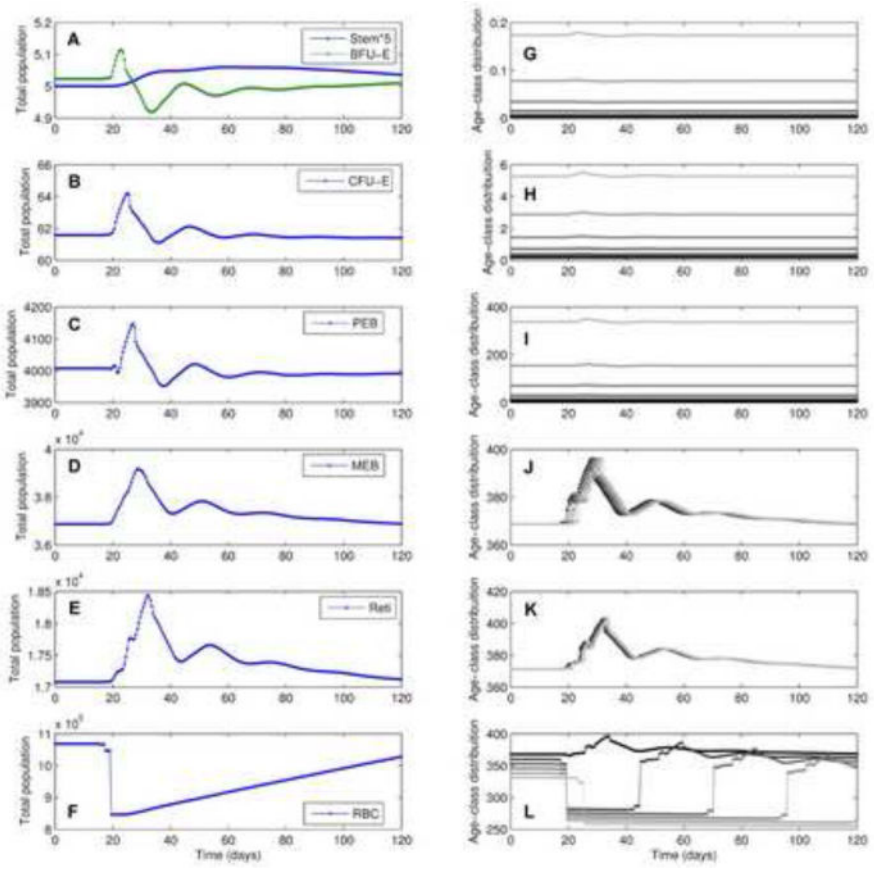

Fig. 11.

Simulation results for a DRE implementation of Schrim and collaborators erythrpoietic model [27] in response to malaria induced anemia (parasitemia levels shown in Figure 12). Panels A–F, show the total numbers of cells present in each pool (Stem (multiplied by 5 for visual ease), BFU-E, CFU-E, PEB, MEB, Reti and RBC). The right panels (G–L) show 6 evenly distributed age-classes of each of the pools shown on the left panels. Panel G shows 6 of the age-classes of BFU-E cells, as stem cells do not have age-classes in this implementation. Age-classes are shown in a black to gray gradient where younger age-classes are shown in dark and older in lighter shades of gray. As the anemia develops between days 5–20, RBCs numbers decline and erythropoietic production increases, leading to an increase in all of the precursor cell pools.

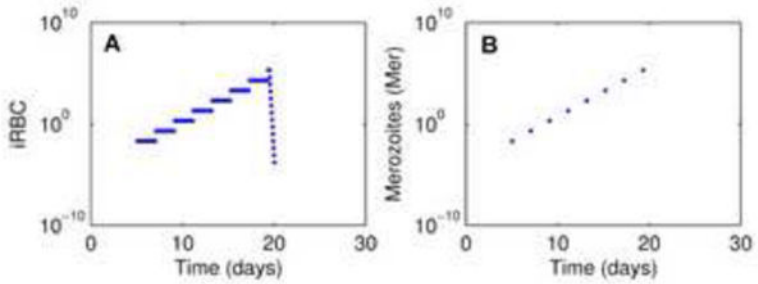

Fig. 12.

Simulation of the parasitemia levels of a malaria infection starting at day 5 with 1 merozoite per 10 million RBCs and terminated by chemical intervention at day 20. Panel A shows the levels of infected RBCs (iRBCs) and panel B the levels of free merozoites. Parasites are assumed to spend one time point (1hr) in their free stage, as merozoites, after which all of them infect RBCs. At the end of their intraerythrotic life cycle, of 48 hours, 16 new merozoites are released from each iRBC. The drug is assumed to kill 4/5 of all iRBCs per hour.

Table 1

Normal transit times in Schirm's RBC model [27] and corresponding numbers of age classes used in our model for simulations with a 1-hour time-step.

Compartment	Normal transit time (h)	Number of age classes
BFU-E	40/0.33	40*3
CFU-E	40	40
PEB	48	48
MEB	100.2	100
Reti	46.4	46
RBC	3061.2	3061
iRBC	24–72†	24–72

†Transit time for infected RBCs is not available in Schirm's model [27], but represents the normal lifespan of an malaria infected human RBC. It depends on the *Plasmodium* species and varies between 1 and 3 days